

Comparative Study of the Influence of μ -c-Si:H, a-Si:H, pm-Si:H and μ -c-SiO_xH as a Passivation Layer on the Performance of HIT n-c-Si Solar Cells

Z. Dahlal¹, F. Hamdache¹, D. Rached¹, W.L. Rahal^{2,3,*}

¹ Laboratoire de Physique des Plasmas, Matériaux Conducteurs et Leurs Applications,
U.S.T.O.M.B. – B.P. 1505, El M'naouar, Oran, Algérie

² Laboratoire d'Analyse et d'Application des Rayonnements, U.S.T.O.M.B. – B.P. 1505, El M'naouar, Oran, Algérie

³ Département de Physique, Faculté des Sciences Exactes et de l'Informatique,
Université Abdelhamid Ibn Badis de Mostaganem, Mostaganem, Algérie

(Received 26 February 2021; revised manuscript received 01 December 2021; published online 20 December 2021)

One of the most important factors limiting the performance of Heterojunction with Intrinsic Thin layer (HIT) c-Si solar cells is the defect density on the surface of crystalline silicon. A numerical modeling has been employed in order to choose the most efficient material as a passivation layer in a HIT c-Si solar cell. We have chosen for this study the following materials: hydrogenated microcrystalline silicon μ -c-Si:H ($E_{g,\mu\text{-Si:H}} = 1.40$ eV), hydrogenated amorphous silicon a-Si:H ($E_{g,a\text{-Si:H}} = 1.84$ eV), hydrogenated polymorphous silicon pm-Si:H ($E_{g,\text{pm-Si:H}} = 1.96$ eV) and hydrogenated microcrystalline silicon oxide μ -c-SiO_xH ($E_{g,\mu\text{-SiO}_x} = 2.5$ eV). The simulation results show that the improvement of the electric field at the emitter with the use of μ -c-Si:H and a-Si:H as a passivation layer makes the power conversion efficiency of the HIT c-Si to increase from 25.42 to 26.34 %. The creation of a potential barrier for photogenerated holes at i-pm-Si:H/n-c-Si and μ -c-SiO_x/n-c-Si junctions drops the efficiency from 23.87 to 3.10 %. This barrier prevents the passage of photogenerated holes towards the emitter which leads to a strong recombination rate of electron-hole pairs and therefore to a decrease in power efficiency. With a band gap of 1.84 eV, hydrogenated amorphous silicon a-Si:H is the most appropriate candidate for the elaboration of a passivation layer on the surface of crystalline silicon for this type of solar cells.

Keywords: Solar cells, HIT, Amorphous silicon, Potential barrier, SCAPS-1D, J-V characteristic.

DOI: [10.21272/jnep.13\(6\).06002](https://doi.org/10.21272/jnep.13(6).06002)

PACS numbers: 73.61.Jc, 71.20.Mq, 88.40.hj, 88.40.jj

1. INTRODUCTION

A HIT (Heterojunction with Intrinsic Thin layer) silicon solar cell was first designed and named by Sanyo Co. Ltd (now Panasonic Co. Ltd) in 1991 [1]. This solar cell is composed of a c-Si silicon wafer as an active layer and ultra-thin amorphous silicon layers as a passivation layer and an emitter. The main advantages of HIT solar cells are their fabrication at low temperature (200 °C), as well as high stable efficiency of crystalline silicon (c-Si) [2-5].

The excellent properties of crystalline silicon allow the HIT solar cell to have an efficiency equal to 26.6 % [6]. Despite the presence of defects in the amorphous matrix, which cause losses affecting the performance of photovoltaic cells (due to the nature of the material gap [7]), materials based on intrinsic hydrogenated amorphous silicon (a-Si:H) are excellent as a passivation layer between an absorber layer (*n*-doped crystalline silicon) and an emitter (*p*-doped hydrogenated amorphous silicon).

In this study, we will compare the quality of surface passivation with several amorphous materials to improve the efficiency of such a solar cell. These materials are: hydrogenated microcrystalline silicon μ -c-Si:H ($E_{g,\mu\text{-Si:H}} = 1.40$ eV), hydrogenated amorphous silicon a-Si:H ($E_{g,a\text{-Si:H}} = 1.84$ eV), hydrogenated polymorphous silicon pm-Si:H ($E_{g,\text{pm-Si:H}} = 1.96$ eV) and hydrogenated microcrystalline silicon oxide μ -c-SiO_xH ($E_{g,\mu\text{-SiO}_x} = 2.5$ eV) [8, 9].

The results of the numerical modelling are obtained using solar cell capacitance simulator SCAPS-1D.

2. INPUT PARAMETERS OF THE STUDIED SOLAR CELL

The structure we proposed to study in this work is a HIT *n*-c-Si (ZnO/*p*- μ -c-Si:H/i- μ -c-Si:H/n-c-Si/*n*⁺-c-Si/Al) solar cell shown in Fig. 1.

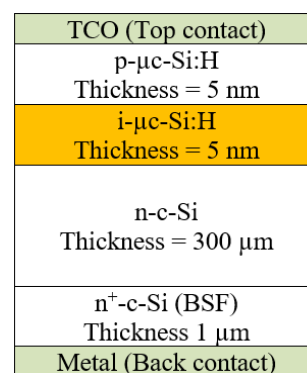


Fig. 1 – Schematic diagram of a HIT *n*-c-Si solar cell

The 300-micron thick *n*-doped c-Si substrate acts as an absorber. Although it is possible to make HIT cells on a *p*-type substrate [10], we have focused in this article on HIT cells on an *n*-type substrate. At the top of the device, we have chosen zinc oxide (ZnO) with a work function equal to 5.2 eV as a transparent conduct-

* leila.rahal@univ-mosta.dz

ing oxide [11]. At the back of the cell, we have used aluminum as a metal with a work function equal to 3.9 eV [12]. The emitter consists of *p*-doped hydrogenated microcrystalline silicon ($\mu\text{-Si:H}$). The addition of an intrinsic $\mu\text{-Si:H}$ layer to the *c*-Si surface is essen-

tial. Without this passivation layer, the concentration of recombination centers is so high that the generated electron-hole pairs (EHP) in the absorber recombine before being extracted from the cell. The parameters used in our simulations are grouped in Table 1 [8, 9].

Table 1 – Principal input parameters of the HIT *n*-*c*-Si solar cell

Parameters	Units	<i>p</i> - $\mu\text{-Si:H}$	<i>i</i> - $\mu\text{-Si:H}$	<i>i</i> - a-Si:H	<i>i</i> - pm-Si:H	<i>i</i> - $\mu\text{-SiO}_x$	<i>n</i> - <i>c</i> -Si	<i>n</i> ⁺ - <i>c</i> -Si (BSF)
<i>d</i>	μm	0.005	0.005	0.005	0.005	0.005	300	1
<i>E_a</i>	eV	1.40	1.40	1.84	1.96	2.50	1.12	1.12
χ	eV	4	4	4	3.95	3.67	4.22	4.22
<i>N_C, N_V</i>	cm^{-3}	2.10^{20}	2.10^{20}	2.10^{20}	2.10^{20}	2.10^{20}	10^{19}	10^{19}
μ_n	cm^2/Vs	32	32	20	20	32	1450	1450
μ_p	cm^2/Vs	8	8	4	12	8	450	450
<i>N_D</i>	cm^{-3}	0	0	0	0	0	10^{17}	10^{21}
<i>N_A</i>	cm^{-3}	10^{19}	0	0	0	0	0	0
<i>N_t</i>	cm^{-3}	10^{21}	10^{14}	10^{14}	10^{14}	10^{14}	10^{10}	10^{10}

To compare the quality of the passivation layer of such a solar cell, we have used various materials. The parameters used for the structure as well as materials as a passivation layer (*a*- Si:H , *pm*- Si:H and $\mu\text{-SiO}_x$) are based on the values taken from the literature [8, 9].

3. SIMULATION MODEL

To accomplish our study, we used the SCAPS one-dimensional numerical simulation software (Solar Cell Capacitance Simulator) [13-15]. Developed by the Department of Electronic and Computer Systems (ELIS) at the University of Gent in Belgium, SCAPS-1D was originally designed for the CIS, CdTe and CIGS family cells. However, a number of extensions have been developed to become applicable to crystalline *c*-Si and amorphous *a*- Si:H solar cells.

SCAPS-1D simultaneously solves the Poisson equation (Eq. (3.1)) and the continuity equations for free electrons and free holes (Eq. (3.2) and Eq. (3.3)) using finite differences and the Newton-Raphson method [16]

$$\frac{\partial^2 \Psi(x)}{\partial x^2} = -\frac{\rho(x)}{\varepsilon}, \quad (3.1)$$

$$G(x) - R(p(x), n(x)) - \frac{1}{q} \frac{\partial j_{n(x)}}{\partial x} = 0, \quad (3.2)$$

$$G(x) - R(p(x), n(x)) - \frac{1}{q} \frac{\partial j_{p(x)}}{\partial x} = 0, \quad (3.3)$$

where $\Psi(x)$ is the electrostatic potential, $\rho(x)$ is the space charge density in the semiconductor, $\varepsilon(x)$ is the dielectric permittivity of the semiconductor, $J_n(x)$ is the electron current, $J_p(x)$ is the hole current, q is the electron charge, $G(x)$ is the net optical generation of free electron-hole pairs per unit volume, $R(x)$ is the net recombination of free carriers per unit volume.

4. RESULTS AND DISCUSSION

Under illumination AM 1.5 and at a temperature of 25 °C, we obtained for a HIT *n*-*c*-Si composed of $\mu\text{-Si:H}$ as a passivation layer ($Eg_{\mu\text{-Si:H}} = 1.40$ eV): short-circuit current density $J_{sc} = 39.31$ mA/cm², open-circuit voltage $V_{oc} = 0.79$ V, Fill Factor FF = 81.26 and efficiency

$\eta = 25.41$ %. Fig. 2 shows the evolution of the band diagram of this cell.

The results of modeling the current-voltage curves *J-V* at 100 mW/cm⁻² of AM 1.5 light, as a function of $\mu\text{-Si:H}$, *a*- Si:H , *pm*- Si:H and $\mu\text{-SiO}_x$ as a passivation layer, are shown in Table 2.

According to Table 2, the efficiencies of cells formed from $\mu\text{-Si:H}$ and *a*- Si:H increase from 25.41 to 26.34 %, while for those made up of *pm*- Si:H and $\mu\text{-SiO}_x$, the efficiencies drop. They are equal to 23.87 % and 3.10 %, respectively. V_{oc} and J_{sc} follow the same drift as the efficiency η . In fact, V_{oc} goes from 0.82 to 0.79 V and J_{sc} goes from 39.37 to 39.31 mA/cm².

For cells made of a material with a wide band gap ($\mu\text{-SiO}_x$), V_{oc} drops to 0.68 V and J_{sc} to 32.12 mA/cm².

Fig. 3 shows the electric field variation for *i*- $\mu\text{-Si:H}$, *i*- a-Si:H , *i*- pm-Si:H and *i*- $\mu\text{-SiO}_x$ materials used as a passivation layer in a HIT *n*-*c*-Si solar cell. An improvement in this electric field clarifies the increase in η , V_{oc} and J_{sc} for cells made from *i*- a-Si:H but does not provide information on a decrease in these parameters for cells made from *i*- pm-Si:H and *i*- $\mu\text{-SiO}_x$. We can notice from Fig. 4 a decrease in the recombination rate of EHP created in the active layer (*n*-*c*-Si). This decrease had a negative impact on the *J-V* characteristic. Indeed, in addition to the fall of V_{oc} and J_{sc} , the FF drops from 81.28 to 14.18 %.

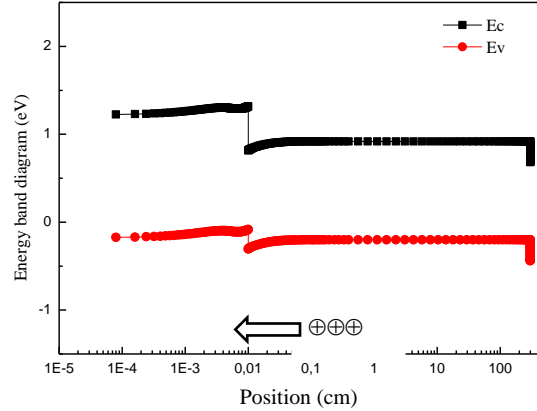


Fig. 2 – Schematic band diagram of a HIT *n*-*c*-Si solar cell: $\text{ZnO}/\mu\text{-Si:H}/\text{i}-\mu\text{-Si:H}/\text{n}-\text{c-Si}/\text{n}^+-\text{c-Si}/\text{Al}$ ($Eg_{\mu\text{-Si:H}} = 1.40$ eV) under solar illumination

Table 2 – Photovoltaic parameters of a HIT n-c-Si solar cell with μc -Si:H, a-Si:H, pm-Si:H, μc -SiO_x as a passivation layer

	V_{oc} (V)	J_{sc} (mA/cm ²)	FF (%)	η (%)
i- μc -Si:H	0.79	39.31	81.26	25.42
i-a-Si:H	0.82	39.37	80.95	26.34
i-pm-Si:H	0.82	39.21	73.56	23.87
i- μc -SiO _x	0.68	32.12	14.18	3.10

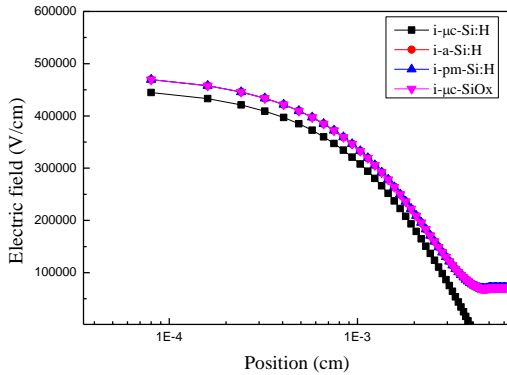


Fig. 3 – The electric field for i- μc -Si:H, i-a-Si:H, i-pm-Si:H and i- μc -SiO_x materials used as a passivation layer in HIT n-c-Si cells as a function of position in the device

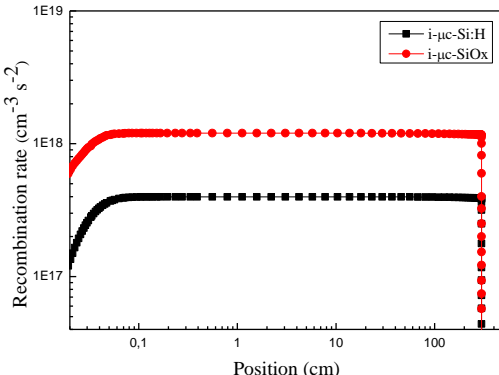


Fig. 4 – Plots of the recombination rate of a HIT n-c-Si solar cell: ZnO/p- μc -Si:H/i- μc -Si:H/n-c-Si/n⁺-c-Si/Al and ZnO/p- μc -SiO_x/n-c-Si/n⁺-c-Si/Al as a function of position in the device

Following these results, we have plotted the energy band diagram of HIT n-c-Si solar cells for i- μc -Si:H and i- μc -SiO_x materials used as a passivation layer.

We can notice from the schematic energy band diagram under illumination (Fig. 5) the creation of a po-

tential barrier for photogenerated holes at the i- μc -SiO_x/n-c-Si junction. This barrier at the level of the valence band will prevent holes from passing to the emitter, which involve a great recombination of EHP and consequently a drop in the efficiency to 3.10 %.

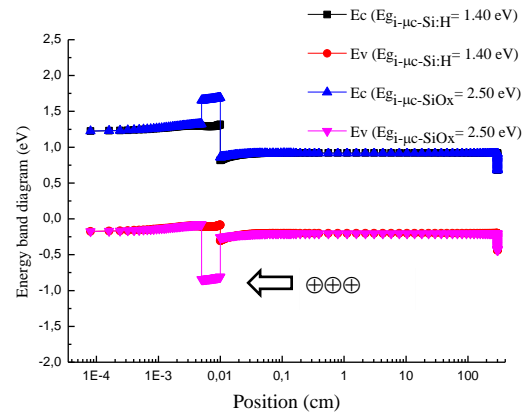


Fig. 5 – Schematic of the energy band diagram of HIT n-c-Si solar cells: ZnO/p- μc -Si:H/i- μc -Si:H/n-c-Si/n⁺-c-Si/Al and ZnO/p- μc -Si:H/i- μc -SiO_x/n-c-Si/n⁺-c-Si/Al under solar illumination

5. CONCLUSIONS

In summary, several materials have been used as a passivation layer in HIT c-Si solar cells. The efficiency of cells with i- μc -Si:H and i-a-Si:H increases from 25.41 to 26.34 %, while for cells made up of i-pm-Si:H and i- μc -SiO_x it drops from 23.87 to 3.10 %, respectively. An improvement in the electric field explains the increase in the J-V characteristic for a cell made from i-a-Si:H. A decrease in the recombination rate of EHP created in the active layer (n-c-Si) had a detrimental effect for cells with a wide band gap as a passivation layer (i-pm-Si:H and i- μc -SiO_x). A large μc -SiO_x gap causes the creation of a potential barrier for photogenerated holes at the i- μc -SiO_x/n-c-Si junction, thus preventing the passage of holes towards the emitter, which leads to strong recombination of EHP and therefore a decrease in efficiency.

ACKNOWLEDGEMENTS

The authors would like to acknowledge Dr. Marc Burgelman at the University of Gent, Belgium for providing the SCAPS-1D simulator.

REFERENCES

- S. Chowdhury, M. Kumar, S. Dutta, J. Park, J. Kim, S. Kim, M. Ju, Y. Kim, Y. Cho, E. Cho, J. Yi, *New Renew. Energy* **15** No 3, 36 (2019).
- S. De Wolf, A. Descoeuilles, Z.C. Holman, C. Ballif, *Green* **2**, 7 (2012).
- T. Ishii, K. Otani, T. Takashima, S. Kawai, *Sol. Energy Mater. Sol. C* **95**, 386 (2011).
- N. Aste, C. Del Pero, F. Leonforte, *Sol. Energy* **109**, 1 (2014).
- F. Azzemou, D. Rached, W.L. Rahal, *Optik* **217**, 164802 (2020).
- M.A. Green, E.D. Dunlop, D.H. Levi, J. Hohl-Ebinger, M. Yoshita, A.W.Y. Ho-Baillie, *Prog. Photovolt.: Res. Appl.* **27** No 7, 565 (2019).
- W.L. Rahal, D. Rached, *J. Nano-Electron. Phys.* **9** No 4, 04001 (2017).
- P. Chatterjee, P. Roca i Cabarrocas, *AIP Adv.* **8**, 015115 (2018).
- D. Rached, H.M. Yssaad, *Acta Phys. Pol. A* **127** No 3, 767 (2015).
- D. Rached, H. Madani Yssaad, W.L. Rahal, *J. Nano-Electron. Phys.* **10** No 5, 05012 (2018).
- O. Tosoni, Conception, élaboration et intégration d'électrodes transparentes optimisées pour l'extraction des charges dans des dispositifs photovoltaïques, Ph.D. Thesis (Université de Grenoble: France: 2013).
- J. Hözl, F.K. Schulte, G. Höhler (Ed.), *Work Functions of Metals*, in Solid Surface Physics (Springer-Verlag: Berlin: 1979).

13. M. Burgelman, J. Verschraegen, S. Degrave, P. Nollet, *Prog. Photovolt. Res. Appl.* **12**, 143 (2004).
14. J. Verschraegen, M. Burgelman, *Thin Solid Films* **515**, 6276 (2007).
15. K. De Cock, S. Khelifi, M. Burgelman, *Thin Solid Films* **519**, 7481 (2011).
16. T. Belaroussi, D. Rached, W.L. Rahal, F. Hamdache, *J. Nano-Electron. Phys.* **12** No 5, 05023 (2020).

Порівняльне дослідження впливу μ c-Si:H, a-Si:H, pm-Si:H та μ c-SiO_x як пасивуючого шару на продуктивність сонячних елементів HIT n-c-Si

Z. Dahlal¹, F. Hamdache¹, D. Rached¹, W.L. Rahal^{2,3}

¹ *Laboratoire de Physique des plasmas, Matériaux Conducteurs et leurs Applications, U.S.T.O.M.B. – B.P. 1505, El M'naouar, Oran, Algérie*

² *Laboratoire d'Analyse et d'Application des Rayonnements, U.S.T.O.M.B. – B.P. 1505, El M'naouar, Oran, Algérie*

³ *Département de Physique, Faculté des Sciences Exactes et de l'Informatique, Université Abdelhamid Ibn Badis de Mostaganem, Mostaganem, Algérie*

Одним з найважливіших факторів, які обмежують продуктивність сонячних елементів c-Si на основі гетеропереходу з внутрішнім тонким шаром (HIT), є густота дефектів на поверхні кристалічного кремнію. Чисельне моделювання було використано для вибору найбільш ефективного матеріалу як пасивуючого шару в сонячному елементі HIT c-Si. Для дослідження ми вибрали такі матеріали: гідрогенізований мікрокристалічний кремній μ c-Si:H ($E_{g,\mu\text{-Si:H}} = 1,40$ eV), гідрогенізований аморфний кремній a-Si:H ($E_{g,a\text{-Si:H}} = 1,84$ eV), гідрогенізований поліморфний pm-Si:H ($E_{g,pm\text{-Si:H}} = 1,96$ eV) і гідрогенізований мікрокристалічний оксид кремнію μ c-SiO_x:H ($E_{g,\mu\text{-SiO}_x\text{:H}} = 2,5$ eV). Результати моделювання показують, що посилення електричного поля на випромінювачі з використанням μ c-Si:H та a-Si:H як пасивуючого шару призводить до збільшення ефективності перетворення енергії сонячного елементу HIT c-Si з 25,42 до 26,34 %. Створення потенційного бар'єру для фотогенерованих дірок на переходах i-pm-Si:H/n-c-Si та μ c-SiO_x/n-c-Si знижує ефективність з 23,87 до 3,10 %. Цей бар'єр перешкоджає проходження фото-генерованих дірок до емітера, що призводить до збільшення швидкості рекомбінації електронно-діркових пар і, отже, до зниження енергетичної ефективності. З шириною забороненої зони 1,84 eV гідрогенізований аморфний кремній a-Si:H є найбільш підходящим кандидатом для створення пасивуючого шару на поверхні кристалічного кремнію для цього типу сонячних елементів.

Ключові слова: Сонячні елементи, HIT, Аморфний кремній, Потенціальний бар'єр, SCAPS-1D, Характеристика *J-V*.